

A BENDING MAGNET WITH NONSATURATING SHIMMING

by

B. Hedin

Stanford Linear Accelerator Center

(On leave from CERN, Geneva, Switzerland)

September 1963

Technical Report

Prepared Under

Contract AT(04-3)-400

for the USAEC

San Francisco Operations Office

REFERENCE USE

TABLE OF CONTENTS

	Page
I. Introduction and summary	1
II. Rectangular pole with return yoke	1
III. Rectangular pole with distant return yoke	5
IV. Inhomogeneity of field near corner	6
V. Shimming to improve homogeneity	10
VI. Rounding of corner	12
VII. Limited pole width	14
VIII. End effects	15
IX. Comparison with window type magnet	18
Appendix: Design of 3 degree bending magnet	19
A. Requirements	19
B. Main magnet dimensions	20
C. Magnetization curves	22
D. Flux-values in pole and yoke	25
E. Optimizing dimensions	28

I. INTRODUCTION AND SUMMARY

In a magnet with rectangular poles, the field falls off towards the sides even if the permeability would be infinitely large in the poles. At the sharp corners, the flux density will however be infinitely high such that all materials saturate even at low fields in the gap. This saturation will result in an even more pronounced drop of the field in the gap. By adding iron at the corners and reducing the gap there (a procedure called shimming) the homogeneous region of the field can be enlarged. The theoretical shape of such shims has been calculated by M. E. Rose¹ for infinite permeability. Other calculations have taken the saturation into account for one particular field strength in the gap.

To get a field shape that is essentially independent of the field strength in the gap up to a level where the entire poles start to saturate, one must have the shims rounded with sufficient radius to avoid local saturation. The design of such shims to produce a wide region of homogeneous field is calculated. An appendix gives calculations for a 3 degree bending magnet for 25 GeV electrons.

II. RECTANGULAR POLE WITH RETURN YOKE

The field near the edge of a rectangular pole with half gap h and with a return yoke at distance d can be found by Schwarz's transformation (see Figs. 1a and 1b). We have the potential functions:

$$Z = x + jy$$

$$W = U + jV = \frac{V_0}{\pi} \ln(\xi/a) \quad (1)$$

$$\xi = \rho \cdot e^{j\varphi} = \rho \cos \varphi + j\rho \sin \varphi$$

At $\xi = 0$ we have an angle = 0

$\xi = b$ we have an angle = $\pi/2$

$\xi = -a$ we have an angle = $3\pi/2$

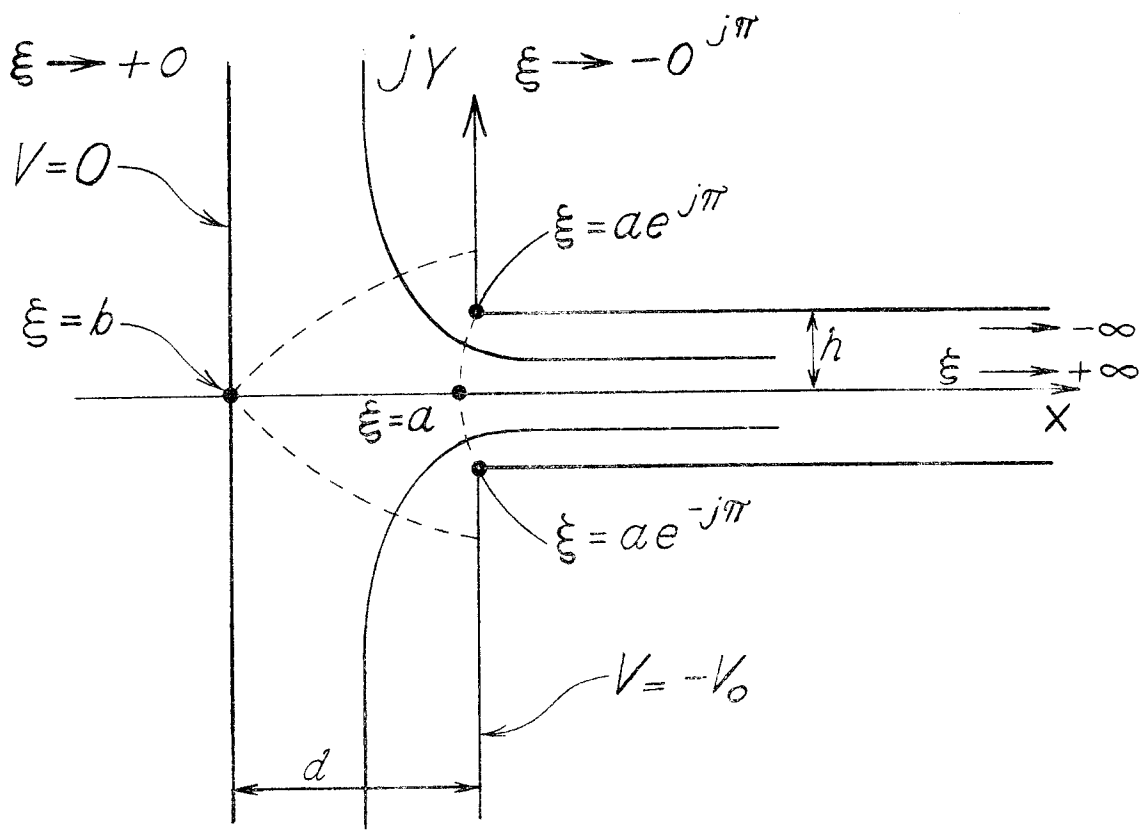


FIG. 1a

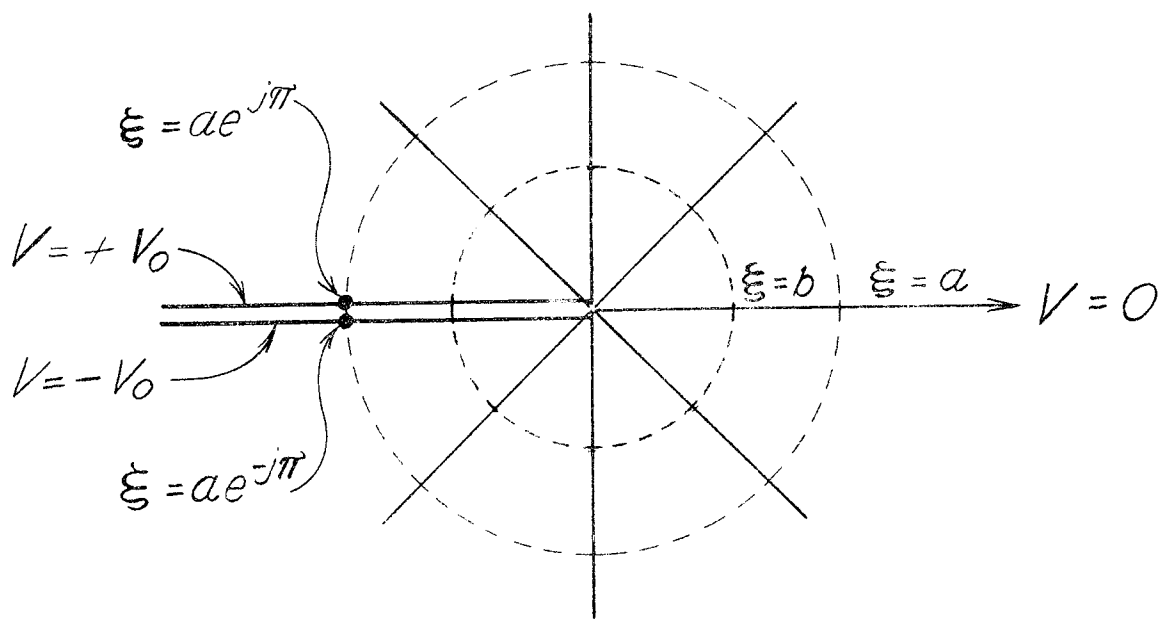


FIG. 1b

This leads to

$$\frac{dZ}{d\xi} = A\xi^{-1} (\xi - b)^{\frac{1}{2}-1} (\xi + a)^{\frac{3}{2}-1} \quad (2)$$

$$Z = A \int \sqrt{\frac{\xi + a}{\xi - b}} \frac{d\xi}{\xi} = A \int \frac{\xi + a}{\sqrt{(\xi + a)(\xi - b)}} \frac{d\xi}{\xi}$$

This integral can be solved by the substitution

$$u = \frac{\sqrt{\xi + a}}{\sqrt{\xi - b}} ; d\xi = - \frac{a + b}{(u^2 - 1)^2} 2u du$$

$$\xi = \frac{bu^2 + a}{u^2 - 1} ; \xi + a = \frac{a + b}{u^2 - 1} u^2 ; \xi - b = \frac{a + b}{u^2 - 1}$$

$$Z = -2A \left\{ \int \frac{du}{u^2 - 1} + \frac{a}{b} \int \frac{du}{u^2 + a/b} \right\} \quad (3)$$

$$Z = A \left\{ \ln \frac{u+1}{u-1} - 2\sqrt{\frac{a}{b}} \tan^{-1} \left(u \sqrt{\frac{b}{a}} \right) \right\} + C \quad (4)$$

The values of A and C are found from the conditions:

$$\left. \begin{aligned} Z(\xi = -a) &= jh \\ Z(\xi = b) &= -d \end{aligned} \right\}$$

Or:

$$A = \frac{h}{\pi}$$

$$\sqrt{\frac{a}{b}} = \frac{d}{h}$$

$$C = 0$$

Depending on the value of ξ different expressions should be used.

For $b < \xi < +\infty$:

$$Z = \frac{h}{\pi} \ln \frac{1 + \sqrt{\frac{1 - b/\xi}{1 + a/\xi}}}{1 - \sqrt{\frac{1 - b/\xi}{1 + a/\xi}}} - \frac{2d}{\pi} \tan^{-1} \left(\sqrt{\frac{\xi/a + 1}{\xi/b - 1}} \right) \quad (5)$$

For $-\infty < \xi < -a$:

$$Z = jh + \frac{h}{\pi} \ln \frac{1 + \sqrt{\frac{1 + a/\xi}{1 - b/\xi}}}{1 - \sqrt{\frac{1 + a/\xi}{1 - b/\xi}}} - \frac{2d}{\pi} \tan^{-1} \left(\sqrt{\frac{\xi/a + 1}{\xi/b - 1}} \right) \quad (6)$$

For $-a < \xi < 0$:

$$Z = 2 \frac{jh}{\pi} \tan^{-1} \sqrt{\frac{b - \xi}{a + \xi}} + \frac{jd}{\pi} \ln \frac{1 + \sqrt{\frac{1 + \xi/a}{1 - \xi/b}}}{1 - \sqrt{\frac{1 + \xi/a}{1 - \xi/b}}} \quad (7)$$

For $0 < \xi < b$:

$$Z = 2 \frac{jh}{\pi} \tan^{-1} \sqrt{\frac{b - \xi}{a + \xi}} + \frac{jd}{\pi} \ln \frac{1 + \sqrt{\frac{1 - \xi/b}{1 + \xi/a}}}{1 - \sqrt{\frac{1 - \xi/b}{1 + \xi/a}}} - d \quad (8)$$

For complex values of ξ and u one can use any one of the expressions (4) to (8) together with

$$\tan^{-1} (A + jB) = \frac{1}{2} \left[\tan^{-1} \frac{A}{1 + B} + \tan^{-1} \frac{A}{1 - B} \right] + \frac{j}{4} \ln \frac{(1 + B)^2 + A^2}{(1 - B)^2 + A^2}$$

and

$$\ln (A + jB) = \frac{1}{2} \ln (A^2 + B^2) + j \tan^{-1} (B/A)$$

III. RECTANGULAR POLE WITH DISTANT RETURN YOKE

For $d \gg h$ and $|y| \ll d$ we can put $u = \sqrt{1 + a/\xi}$ and get from (4)

$$Z = \frac{h}{\pi} \ln \frac{\sqrt{1 + a/\xi} + 1}{\sqrt{1 + a/\xi} - 1} - \frac{2}{\pi} h \sqrt{1 + a/\xi} \quad (9)$$

This expression gives real Z for $0 < \xi < +\infty$. For $-\infty < \xi < -a$:

$$Z = jh + \frac{h}{\pi} \ln \frac{1 + \sqrt{1 + a/\xi}}{1 - \sqrt{1 + a/\xi}} - \frac{2}{\pi} h \sqrt{1 + a/\xi} \quad (10)$$

For $-a < \xi < 0$:

$$A = jh - \frac{2jh}{\pi} \tan^{-1} \sqrt{-1 - a/\xi} + \frac{2}{\pi} h \sqrt{-1 - a/\xi} \quad (11)$$

For a point $x = 0$ and $y = y_1 \gg h$ we have $|a/\xi| \gg 1$ and

$$y_1 = h \left[1 - 1 + \frac{2}{\pi} \sqrt{-a/\xi_1} \right] = \frac{2}{\pi} h \sqrt{-a/\xi} \quad (12)$$

or

$$\xi_1/a = -\frac{4}{\pi^2} h^2/y_1^2 \quad U_1 = \frac{V_0}{\pi} \ln \left(\frac{2}{\pi} h/y_1 \right) \quad (13)$$

For another point $y = h$ $x = x_2 \gg h$ we have $\xi/a \rightarrow -\infty$ and

$$x_2 \approx \frac{h}{\pi} \ln \frac{2 + \frac{1}{2} \frac{a}{\xi_2}}{1 - 1 + \frac{1}{2} \frac{a}{\xi_2}} - \frac{2}{\pi} h - \frac{2}{\pi} h \frac{1}{2} \frac{a}{\xi_2} \approx \frac{h}{\pi} \left[2 \ln 2 - 2 + \ln(\xi_2/a) \right] \quad (14)$$

$$\ln \xi_2/a = 2 - 2 \ln 2 + \pi x_2/h \quad U_2 = V_0 \left[\frac{2}{\pi} - \frac{2}{\pi} \ln 2 + x_2/h \right] \quad (15)$$

The expressions (12) and (13) give us the flux per unit length between the two points:

$$U_2 - U_1 = V_0 \left[\frac{2}{\pi} - \frac{2}{\pi} \ln 2 + x_2/h + \frac{2}{\pi} \ln(y_1/h) \right] \quad (16)$$

$V_0 x_2/h$ represents a homogeneous flux in the gap. $V_0 \frac{2}{\pi} \ln(y_1/h)$ represents a semicircular flux between the sides of the two poles.

$V_0 \left(\frac{2}{\pi} - \frac{2}{\pi} \ln 2 \right)$ is an additional flux that enters near the corner of the pole. The magnitude of this flux is equal to that of a

$$\frac{2}{\pi} (1 - \ln 2) h = 0.195h$$

width of the gap.

IV. INHOMOGENEITY OF FIELD NEAR CORNER

To evaluate the flux density near a rectangular corner we have the following expressions from (1) and (2)

$$\frac{dW}{dZ} = \frac{\partial U}{\partial x} + j \frac{\partial V}{\partial x} = \frac{V_0}{h} \sqrt{\frac{\xi - b}{\xi + a}} \quad (17)$$

$$\frac{\partial V}{\partial y} = \frac{\partial U}{\partial x} = \frac{V_0}{h} \operatorname{Re} \sqrt{\frac{\xi - b}{\xi + a}} \quad (18)$$

$\frac{V_0}{h} = B_0$ is the flux density in the gap well inside the edge. (Fig. 2)

By combining (18) with (5) or (9) one can calculate the corresponding values of $B_y = \partial V / \partial y$ and x (see Fig. 3). Inside the edge, the field is very little affected by the distance d to the return yoke. This part is better drawn in logarithmic scale as in Fig. 4, which gives the quality value $B_0 / (B_0 - B) = Q$ as a function of x/h . For positive

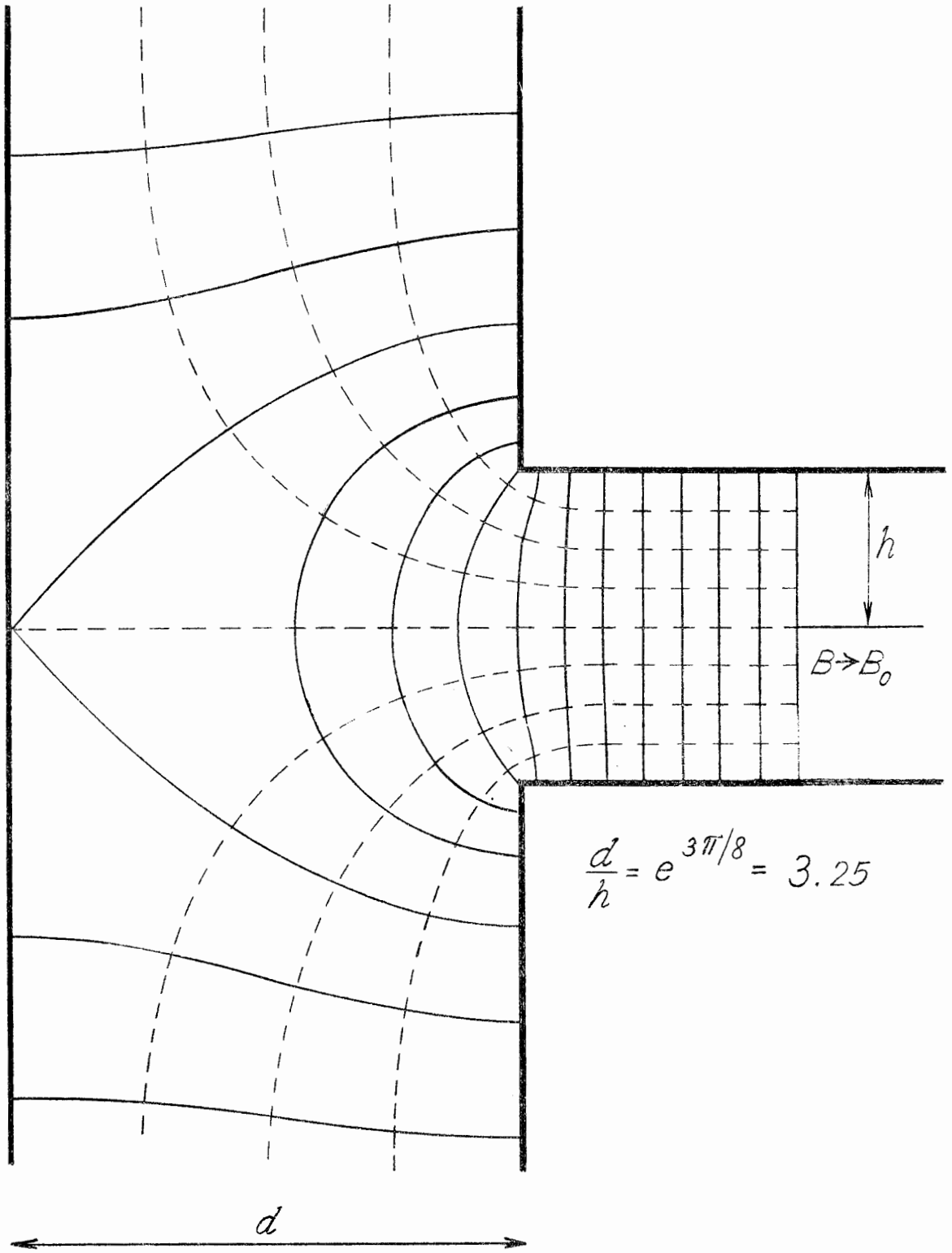


FIG. 2

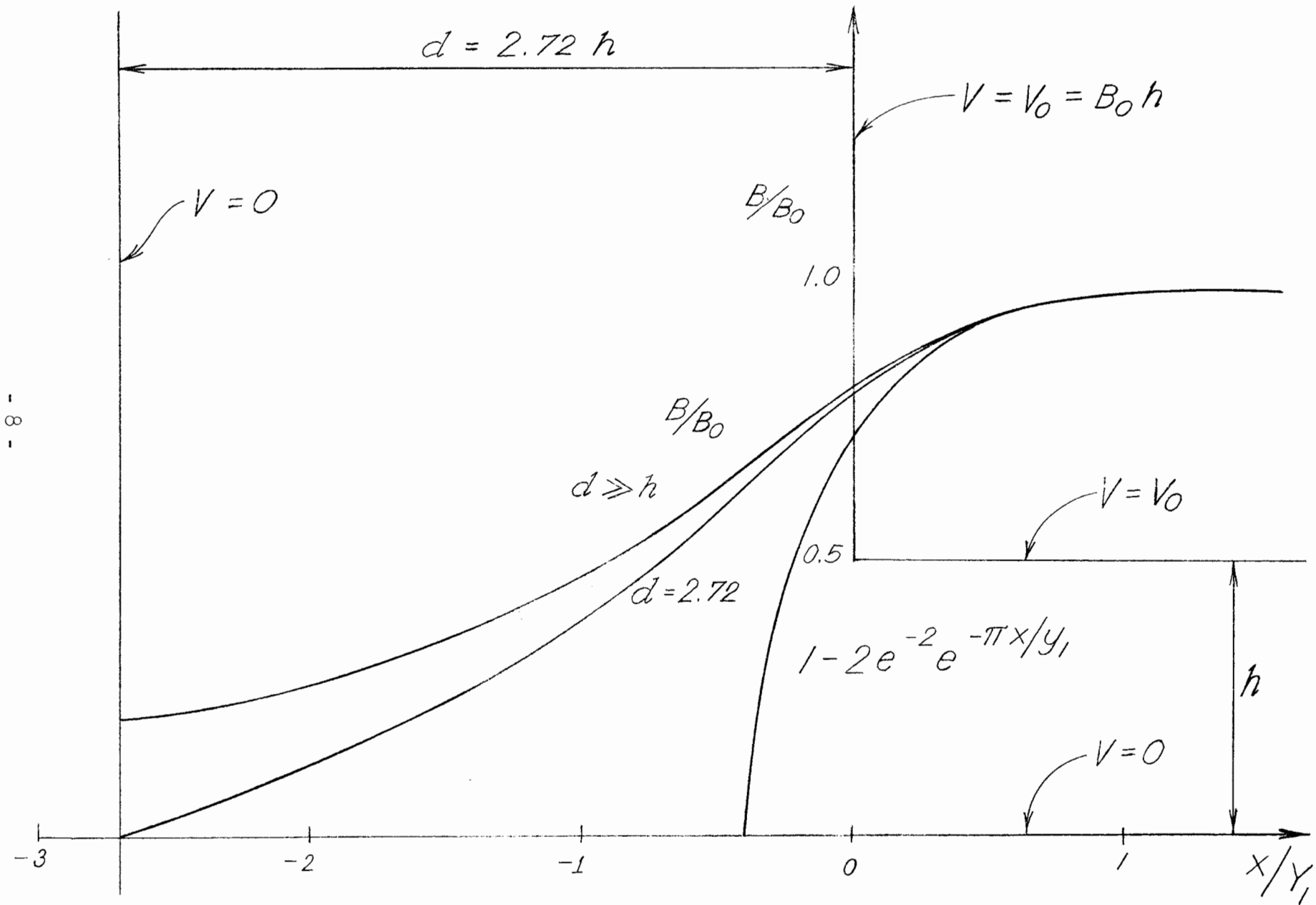


FIG. 3

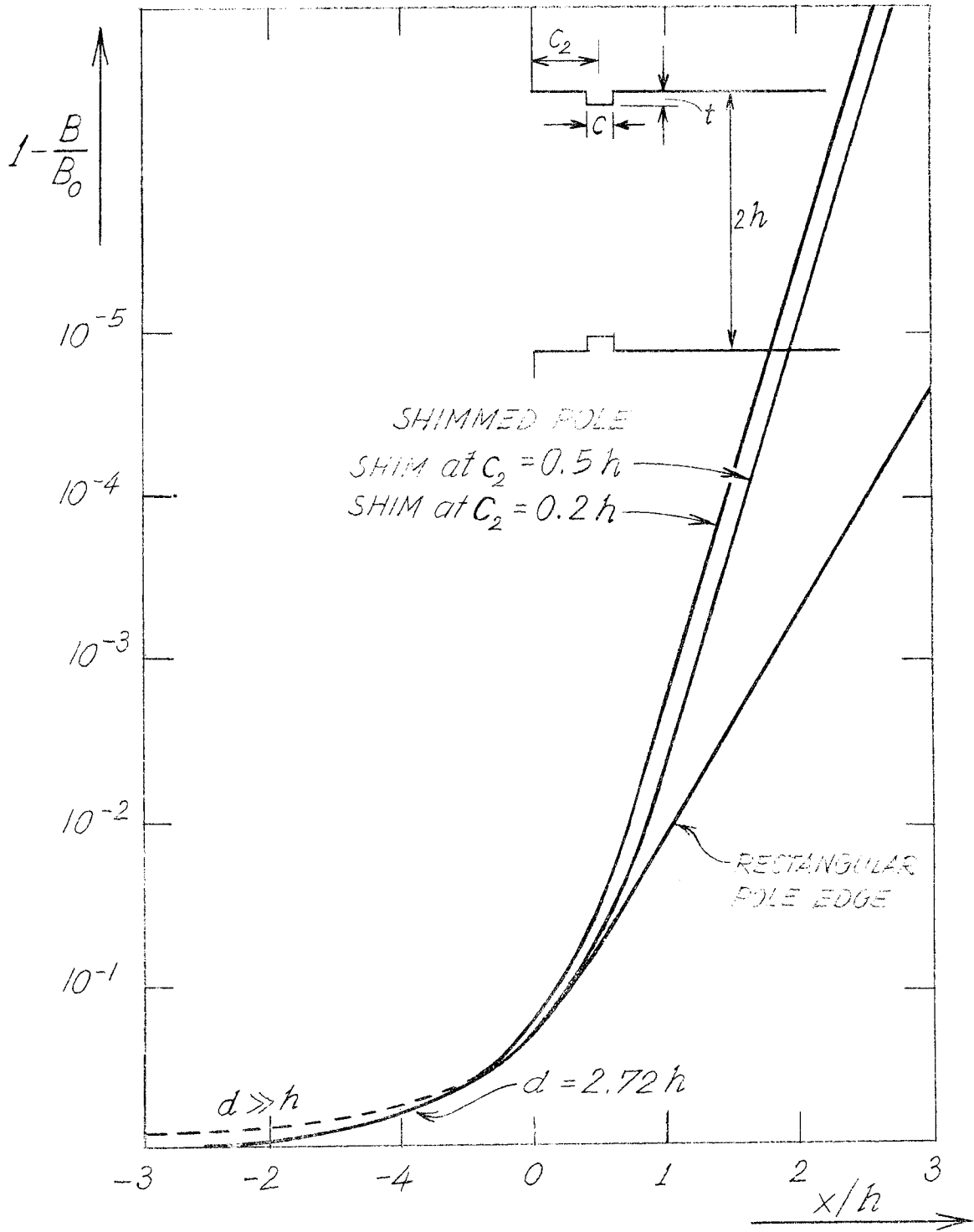


FIG. 4

x the quality approaches

$$Q \approx 0.5e^2 e^{\pi x/h} = 3.7e^{\pi x/h} = \frac{1}{0.27} e^{\pi x/h} \quad (19)$$

To get $Q = 100$, that is 1% less than the maximum field, one has to go more than one-half gap inside the edge. To get 10^{-4} from the maximum field one must go 2.5 half gaps from the edge with unshimmed rectangular poles even if saturation effects can be neglected or are eliminated by rounding the corner.

V. SHIMMING TO IMPROVE HOMOGENEITY

A thin shim of width c and thickness t on the pole surfaces of a magnet with flat poles, gap $2h$ and $H_0 h$ ampere turns per pole will produce an increase in the field, ΔH , in the midplane

$$\Delta H = \frac{ctH_0}{h^2} \frac{\mu_r - 1}{\mu_r} \cdot \frac{h}{4c} \left[\tan h \left(\frac{\pi c + x_1}{2h} \right) + \tan h \left(\frac{\pi c - x_1}{2h} \right) \right] \quad (20)$$

For $c \ll h$ and $\mu_r \gg 1$

$$\Delta H = \frac{ctH_0}{h^2} \frac{\pi/2}{\cosh \frac{\pi x_1}{h} + 1} \quad (21)$$

The corresponding potential function is:

$$W = \frac{ctH_0}{2h} \tan h \frac{\pi Z}{2h} \quad (21a)$$

For the large values x_1 :

$$\Delta H/H_0 \approx \frac{ct}{h^2} \cdot \pi e^{-\pi x_1/h} \left(1 - 2e^{-\pi x_1/h}\right) \quad (22)$$

$$\Delta U = W\left(\begin{matrix} x = +\infty \\ y = 0 \end{matrix}\right) - W\left(\begin{matrix} x = -\infty \\ y = 0 \end{matrix}\right) = \frac{ctH_0}{h} = \frac{ct}{h^2} V_0 \quad (22a)$$

If the shims are a distance c_2 inside the edge (see Fig. 4), one finds the resulting field from (19) and (22)

$$B/B_0 \approx \left(1 - \frac{1}{Q}\right) \left[1 + \pi \frac{ct}{h^2} e^{-\frac{\pi}{h}(x-c_2)}\right] \quad (23)$$

or for $1/Q = 0.27e^{-\pi x/h} \ll 1$:

$$B/B_0 \approx 1 - 0.27e^{-\pi x/h} + \pi \frac{ct}{h^2} e^{\pi c_2/h} e^{-\pi x/h} \quad (24)$$

The error in the field is minimized if

$$\pi \frac{ct}{h^2} e^{\pi c_2/h} = 0.27 \quad (25)$$

The resulting field quality for $c_2 = 0.2h$ and for $c_2 = 0.5h$ is drawn in Fig. 4. For $x \gg (h + c_2)$ one finds from (22) and (25):

$$\frac{1}{Q} = 1 - \frac{B}{B_0} \approx 0.54e^{\pi c_2/h} e^{-2\pi x/h} \quad (26)$$

An error of less than 10^{-4} is achieved 1.6 half gaps from the edge.

VI. ROUNDING OF CORNER

In order to limit the maximum flux density, one can round off the corner in many different ways. This means that iron is removed in some places and added in others. The field quality is practically unchanged if

$$\int t(x)e^{\pi x/h} dx = \frac{0.27}{\pi} h^2 = 0.086 h^2 \quad (27)$$

This formula can be found from comparison with Eq. (25). Figure 5 shows one shape. By graphical integration one can verify that this shape fulfills Eq. (27). The field shape will closely resemble that of a pole shimmed at $x = 0.8h$ (compare Fig. 4) except close to the corner. The ξ -values and the flux that enters the rectangular corner between the 45° line ($\xi = -a$) and the point $x = 1.088h$, $y = h$ can be found from Eqs. (10) and (1) which give the ξ -value and the U-value respectively. One finds $\xi = -56.2a$ and $U_2 - U_1 = \frac{1}{\pi} V_0 \ln 56.2 = 1.283 V_0$. To this flux must be added the flux of the shims according to Eq. (22a). This is negative and amounts to $-0.079 V_0$. The total flux is then $1.204 V_0$. The length of pole surface where this flux enters is

$$\pi R_2 \frac{45 + 19.8}{180} = 1.132 R_2 = 0.962h$$

The (average) flux density on this surface is then $\frac{1.204}{0.962} = 1.25$ times the flux density in the center of the magnet.

More detailed studies of the field shape at the corner have been made using a series $W = \sum k_n \sin h \frac{n\pi Z}{2h}$ for the potential, and have confirmed these results.*

For a flux density of 1.6 Tesla (=16000 gauss) the flux density at the surface of the iron would be 2.0 Tesla. The relative permeability of ordinary steel castings is 60 or higher at this field. The pole

* The computer programs were made by Sam Howry.

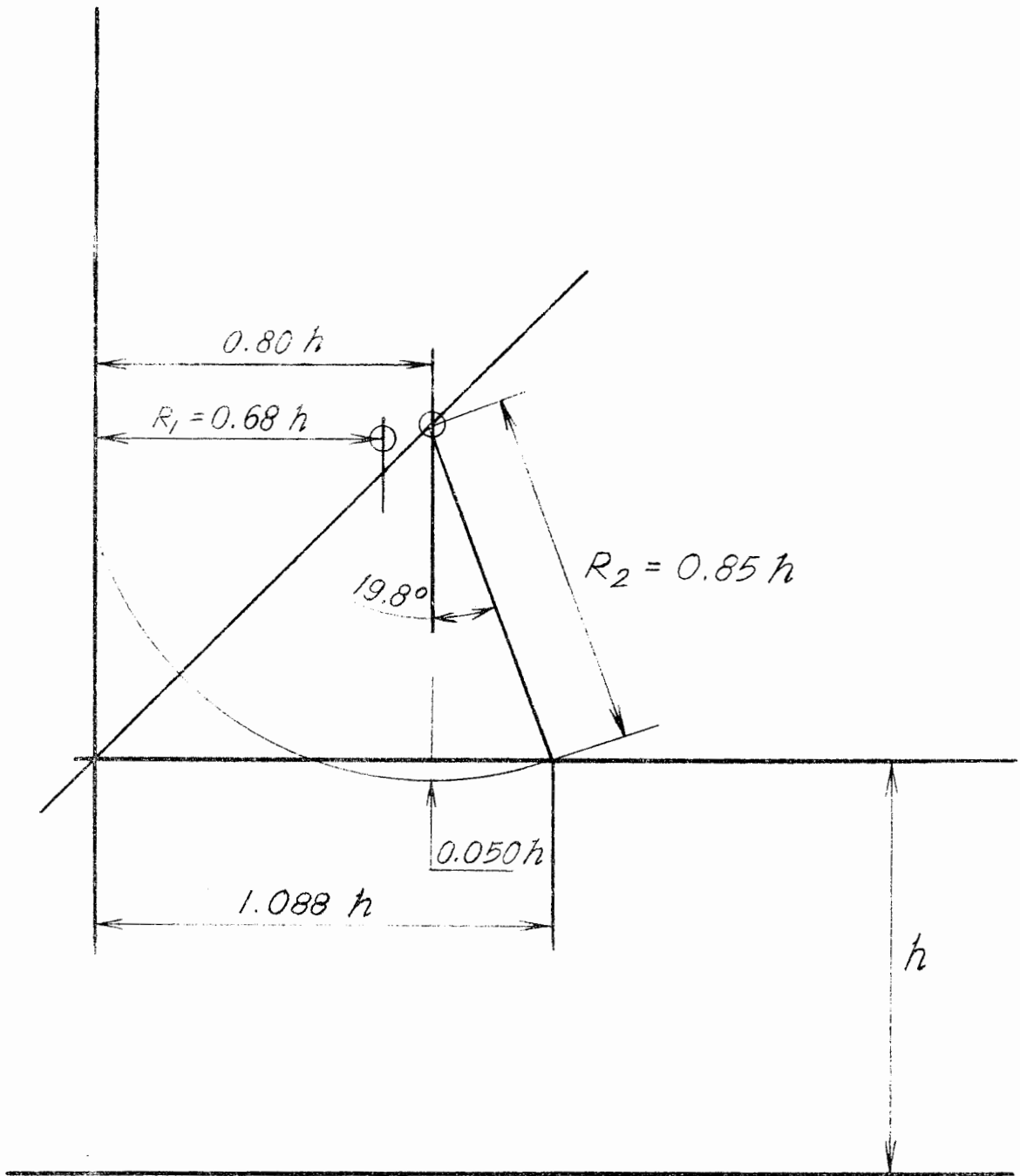


FIG. 5

surface will therefore very nearly be an equipotential of the magnetic field up to around 1.6 Tesla. At higher fields the field shape will change more and more as the iron in the corner saturates.

VII. LIMITED POLE WIDTH

We have seen that the effect of one corner is a reduction in the field strength in the gap given by Eq. (19) or Eq. (26). If the width of the pole is much larger than the half gap h and the coordinate system is transferred to the center of the magnet, one finds for the unshimmed magnet:

$$1 - \frac{B}{B_0} = 0.27 \left[e^{-\frac{\pi}{h}(w-x)} + e^{-\frac{\pi}{h}(w+x)} \right] \quad (28)$$

$$1 - \frac{B}{B_0} = 0.54 e^{-\pi w/h} \cosh(\pi x/h) \quad (28a)$$

and for the shimmed magnet:

$$1 - \frac{B}{B_0} = 0.54 e^{\pi c_2/h} \left[e^{-\frac{2\pi}{h}(w-x)} + e^{-\frac{2\pi}{h}(w+x)} \right] \quad (29)$$

$$1 - \frac{B}{B_0} = 1.08 e^{-\frac{\pi}{h}(2w-c_2)} \cosh(2\pi x/h) \quad (29a)$$

As an example, let us assume a long magnet with 6 cm gap ($h = 3$ cm) and 30 cm wide pole ($w = 15$ cm) shimmed according to Fig. 5 ($c_2 \approx 0.8h$). One finds for x in cm:

$$1 - \frac{B}{B_0} \approx 2.8 \cdot 10^{-13} \cosh(2.1x) \quad (30)$$

B_0 is the field that would be reached if the pole were infinitely wide.

The field in the center is very close to this value. The useful region of the gap for different acceptable field errors can be found from Table I.

TABLE I

$1 - \frac{B}{B_0}$	$(w-x)/h$	$x(\text{cm})$
10^{-5}	2.13	± 8.6
10^{-4}	1.77	± 9.7
10^{-3}	1.36	± 10.9
10^{-2}	0.93	± 12.2

VII. END EFFECTS

The preceding has been devoted to the two-dimensional problem of a very long magnet. At the ends, the field is three-dimensional and not so easy to calculate. Inside the pole edge where the field errors are small it is justified to add the errors caused by the three edges. One can in this manner, with acceptable accuracy, determine the lines where the field strength is for instance 95%, 90% and 85% of the maximum field. These lines will be curved at the corners and will result in a shorter effective length left and right of the center line of the magnet unless proper action is taken.

From measurements on other magnets it is found that the error can be considerably reduced by using a magnetic guardplate that limits the extent of the stray field. A number of lines of constant field strength in the midplane of a magnet with rectangular poles and guardplate are shown in Fig. 6. By making the poles somewhat longer near the corners, that is by adding corner shims, one can readily make the magnetic length constant up to a width of about $2w - 4h$. The best shape of this shim and the field strength in the gap where it starts to saturate is preferably determined by experiments on a prototype magnet.

For the prototype of the 3 degree bending magnets, the ends will be rounded off with a radius of $5h/3$, keeping the profile (see Fig. 7).

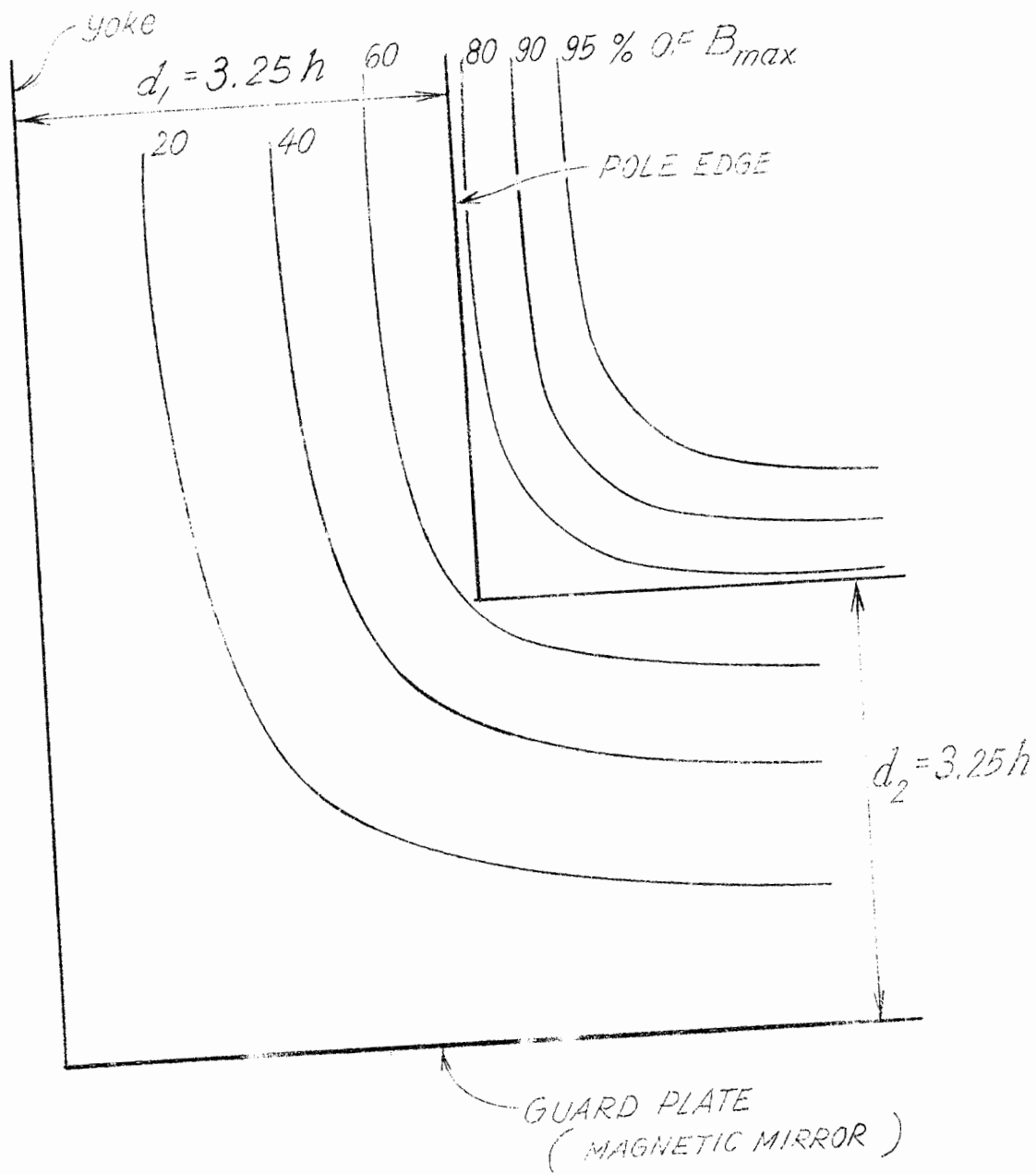


FIG. 6

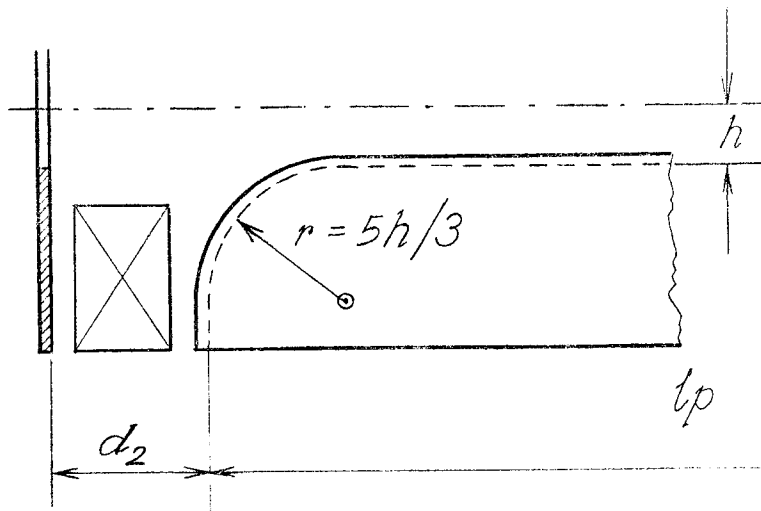
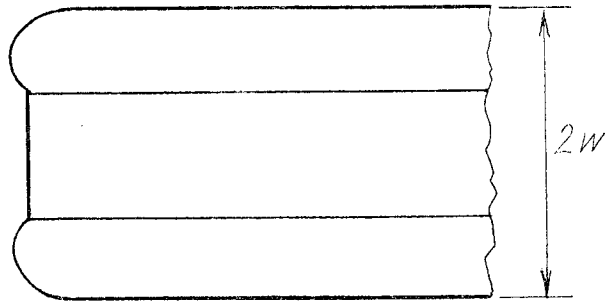
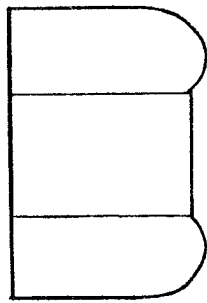


FIG. 7

The distance d_2 is $7.7h$. By plotting the end field ("pencil and rubber method") one finds that the effective length with these dimensions is about $2 \times 0.67n = 1.3h$ longer than the pole length l_p . For a pole length of 300 cm and gap $2h = 6$ cm, one would get an effective length $l_{\text{eff}} = 304$ cm. The higher flux density in the pole at the ends may slightly reduce this effective length. In order to avoid uneven saturation of the yoke along the magnet the yoke members are somewhat longer than l_{eff} .

VIII. COMPARISON WITH WINDOW TYPE MAGNET

A window type magnet has the inherent property of producing a nearly homogeneous field and has no increased flux density at the sides of the useful gap. At the ends of the magnet the problems are the same as with the pole type magnet or rather worse because of the bent-out coil ends.

By the means discussed previously one can achieve comparable homogeneity with a pole type magnet over a wide range of flux density in the gap. The choice between the two types of magnets is then to be made from points of economics and reliability. For equal deflection angle, gap cross section and taking into account the generally higher cost of power for the window type magnet one finds the pole type magnet to be cheaper. For a high power electron beam that may be mis-steered, the coils of the pole type magnet are less exposed. The latter point of view has played an important role in the choice of shimmed pole type magnets for the beam switchyard at the Stanford Two-mile Linear Accelerator.

APPENDIX
DESIGN OF 3 DEGREE BENDING MAGNET

A. REQUIREMENTS

In the beam switchyard of the Stanford Two-mile Linear Accelerator there will be two beams, A and B. The A-beam shall have two deflections of 12 degrees each, useful up to at least 25 GeV electron energy. This requires

$$\int B ds = \frac{25 \cdot 10^9}{3 \cdot 10^8} \cdot \frac{12\pi}{180} = 17.4(\text{T} \cdot \text{m}) = 17.4(\text{Vs/m}) \quad (31)$$

This could be achieved for instance by a single magnet 12 meters long with a flux density $B_0 = 1.45$ teslas (= 14,500 gauss). Such a magnet would, however, be inconveniently long and heavy and is therefore split up into four magnets, each of 3 meters effective length and giving 3 degrees of deflection. This has the additional convenience that each magnet can be straight. The 1.5-degree entrance and exit angles can be accounted for in the setup of the system. One can also with advantage use the same magnet design in the B-beam where two groups of three magnets will be used for 2×6 degree deflection. That would allow this beam to be used up to somewhat higher energies. The aberrations caused by the bending magnet must be small compared with the emittance of the beam from the accelerator. The beam is assumed to have a diameter of $1/4$ inches = 0.6 cm and a divergence of $0.5 \cdot 10^{-5}$ radians. The intensity distribution is gaussian

$$i = i_0 e^{-(r/r_0)^2} \quad (\text{amp/cm}^2) \quad (32)$$

with $r_0 = 0.3$ cm.

The total beam current inside a radius r is:

$$I(r) = \pi r_0^2 i_0 \left[1 - e^{-(r/r_0)^2} \right] \quad (33)$$

This means that when leaving the accelerator, 63% of the beam is contained within a circle of 0.3 cm radius; 98% within 0.6 cm radius. The cross section in the bending magnets is about twice as large, such that 98% of the beam of any one energy is contained within a circle with 1.2 cm radius. Due to the resolution within the magnets the total beam (rather 98%) will be 4.8 cm wide at the exit of the magnet. This beam must be deflected without appreciable loss of quality.

B. MAIN MAGNET DIMENSIONS

The magnets will be made straight; therefore, their width must be increased by an amount

$$\Delta W = \frac{\ell}{2} \frac{1 - \cos \varphi/2}{\sin \varphi/2} \approx \varphi/8 \quad (34)$$

From Eq. (34), for

$$\varphi = 3^\circ = 0.052 \text{ radians}$$

$$\ell = 300 \text{ cm}$$

we find

$$\Delta W \approx 2.0 \text{ cm}$$

The field over a width of $4.8 + 2.0 = 6.8$ cm must cause a difference of deflection $\Delta\varphi$, for four magnets much smaller than the initial divergence, say

$$4\Delta\varphi = 0.1 \cdot 10^{-5} \ll 0.5 \cdot 10^{-5}$$

$$\frac{\Delta\varphi}{\varphi} = 5 \cdot 10^{-6}$$

To accommodate the vacuum tank the gap, $2h$, of the magnet must be 6 cm. With an unshimmed magnet with rectangular pole the required homogeneity could be achieved with a pole width of $6.8 + 7h \approx 28$ cm if

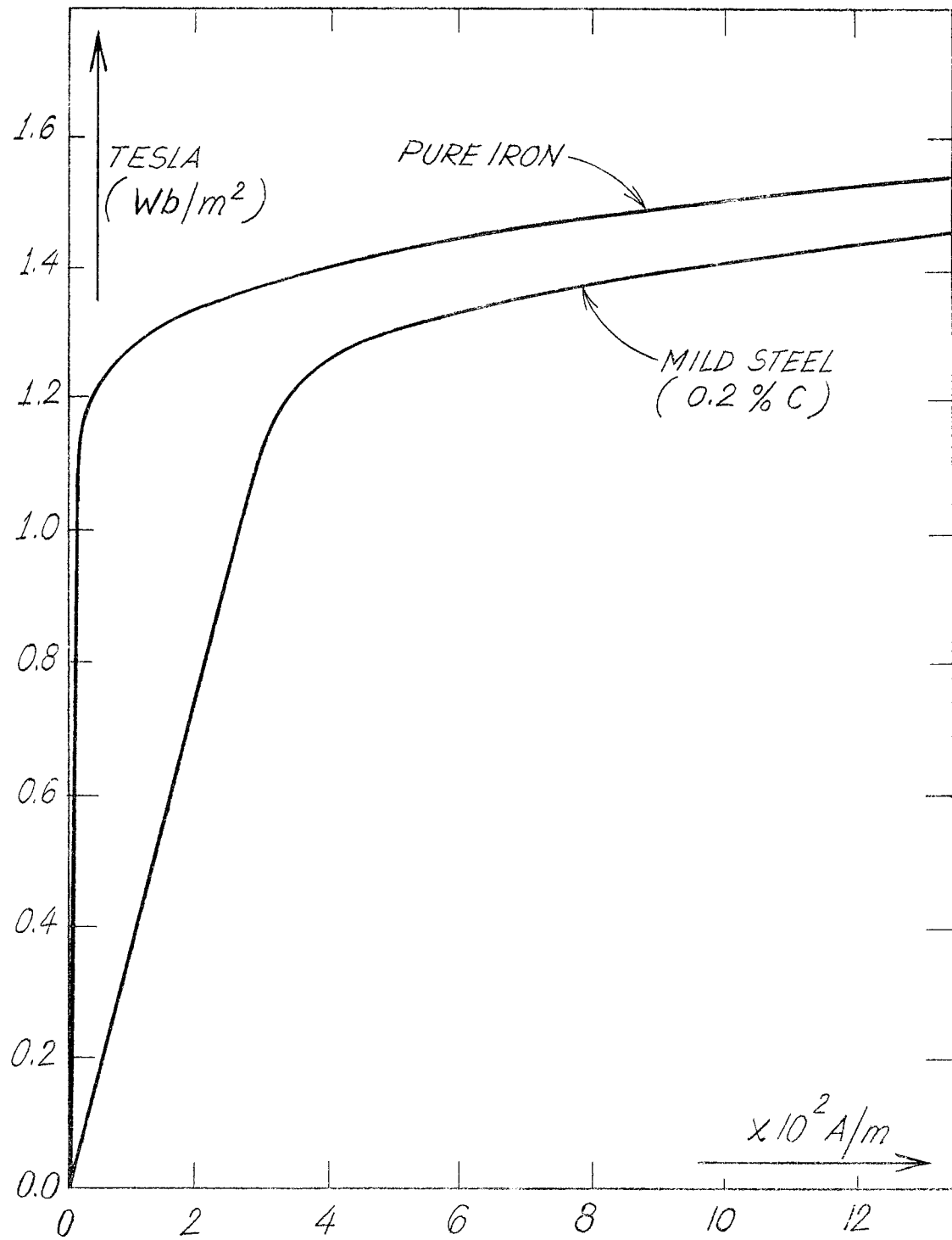


FIG. 8

saturation of edges and corners of the pole could be neglected. In order to allow a margin for misalignment and other imperfections the pole width with nonsaturating shimming was put at 30 cm.

The main dimensions of the magnet are given in Fig. 10. With these dimensions it is possible to calculate the flux in different sections of the iron and then the total number of ampere turns required assuming a given iron quality.

C. MAGNETIZATION CURVES

The effect of small amounts of different elements on the magnetization curves of iron have been studied by Gerold³ and Bozorth.⁴ The alloying elements form compounds that (depending upon whether their melting point is higher or lower than that of pure iron) are deposited in the crystal boundaries or as grains in the pure iron. In a structure with a non-magnetic compound occupying p percent by weight and the iron occupying $100 - p$ percent, one gets a macroscopic flux density and field strength:

$$B = B_i - (B_i - \mu_o H_i) \Sigma p_n k_n \quad (35)$$

$$H = H_i + \frac{1}{\mu_o} (B_i - \mu_o H_i) \Sigma p_n k_n / C \quad (36)$$

Here B_i and H_i represent the values for the pure iron. A good agreement with measurements is achieved if $C = 93$ and k depends on the density of the compound, its solubility in iron, its melting point and crystal shape. For impurities up to about 2% it has been found that the effects of different impurities can be added to find the resulting magnetization curve. Table II gives the values of the constants for some elements.

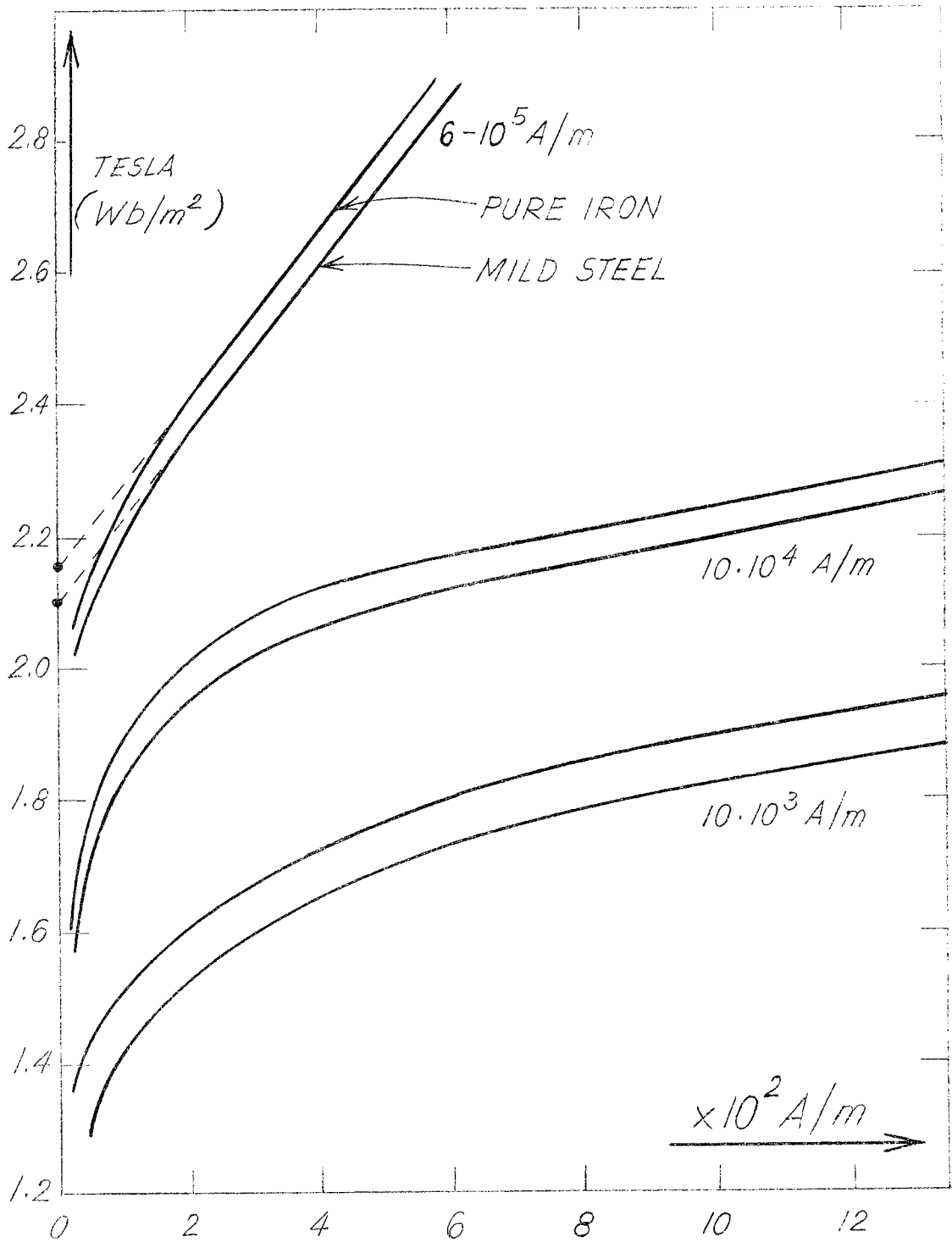


FIG. 9

TABLE II

<u>Element</u>	<u>k</u>
C	0.135
Al	0.029
Mo	0.020
S	0.025
P	0.030
Cr	0.014
Cu	0.008
Mn	0.015
Si	0.014

One sees that carbon has by far the strongest influence. Next in importance are elements such as Al, Mo, S and P which have a detrimental effect on the magnetic properties. A third group of elements has little influence on the magnetic properties. Some of these elements are important to make the steel easy to forge and machine. Another important factor affecting the behavior of the magnet is the homogeneity. The amount of gases such as O_2 and N_2 that are dissolved in iron decreases as the temperature is lowered after casting. The free gases form bubbles unless the steel is "killed" with aluminum or silicon. Impurities have a tendency to agglomerate in the top part of the ingot. About one third of the volume is normally cut off to get rid of most of the impurities. Depending on the source of the ore, wide tolerances on the iron composition can be allowed and give good homogeneity and machinability provided the limits are set as follows:

TABLE III

C	max. 0.12 percent
Total Al + Mo + S + P	max. 0.10 percent
Total Mn + Ni + Cr + Cu + Si	max. 0.70 percent

Such a steel will in average have a magnetization curve close to the one of 0.2 percent carbon steel with no other impurities (see Figs. 8 and 9). These curves show the average of field strength for any flux density approached from higher or lower values. To find the field for the two branches of hysteresis loop for the types of steel considered here, one has to add or subtract about 4000 Σ pk (amperes per meter) or about 100 amperes per meter for a steel with 0.2% C only. In the interesting range above 1.4 tesla little can be gained by lowering the limit of alloying elements, but with too low a carbon content the iron gets so soft that it is difficult to attain close machining tolerances.

D. FLUX-VALUES IN POLE AND YOKE

With the formulas previously derived, Eqs. (16) and (27), and with dimensions from Fig. 10, one finds the flux that enters the pole face at $B_o = 1.45$ teslas from

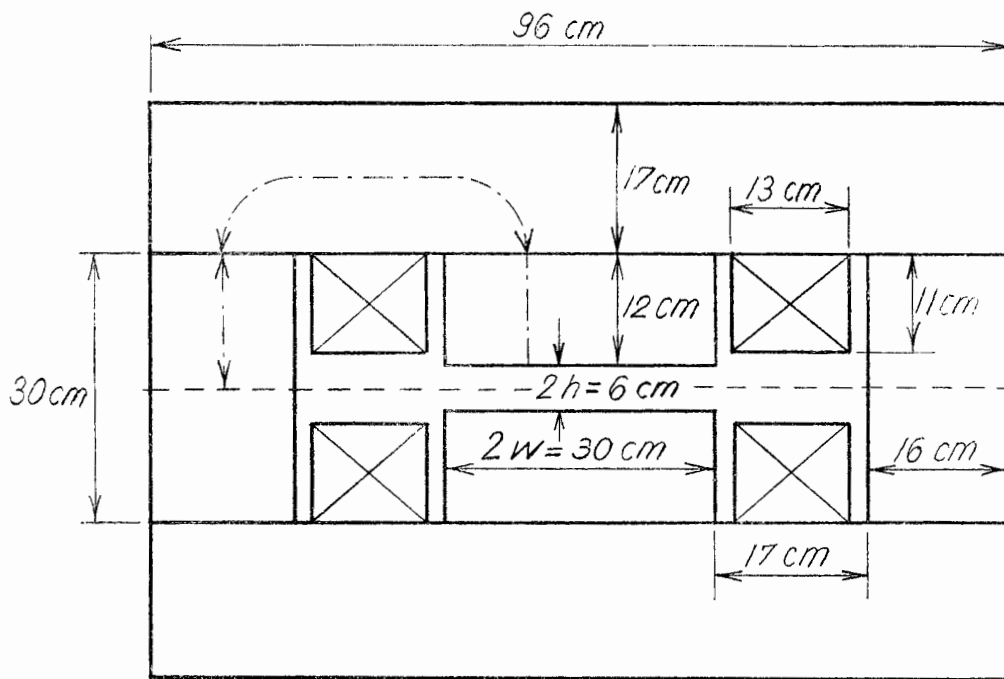
$$\Phi_1 = B_o \ell_{\text{eff}} \cdot h [2 \cdot 0.195 + 2W/h - 2 \cdot 0.079] \quad (37)$$

$$\Phi_1 = 1.45 \cdot 3.00 \cdot 0.030 \cdot 10.232 = 1.332 \text{ Wb}$$

$$\Phi_p(y) = \Phi_1 + 2B_o \ell_{\text{eff}} h \frac{2}{\pi} \ln \frac{y}{h} \quad (38)$$

Equation (38) is valid as far as no appreciable number of ampere turns in the coil is intersected by the flux lines, say up to $y = 11$ cm. This gives a slightly too high value. If this high flux is assumed constant up to the yoke at $y = 15$ cm, one gets a number of ampere turns for the pole close to the real value. When the number of ampere turns for the pole amounts to a large fraction of the total, a more accurate calculation can be made using a constant current density in the winding. Tables IV and V give the results of calculations at two field values.

The coils have been laid out with three double pancakes per coil, 8 turns per layer. This gives 48 turns per coil and requires 755 amperes for 1.45 tesla. The rated current is put 10% higher at 835 amperes.



Length of yoke 310 cm

FIG. 10

TABLE IV

y cm	Part	Area m ²	Φ Weber	B Tesla	H A/m	NI At/pole
0-3	airgap			1.450	$1.154 \cdot 10^6$	34600
3	pole face	0.09	1.332	1.481	$1.6 \cdot 10^3$	} 410
5	pole	0.09	1.417	1.573	$2.7 \cdot 10^3$	
7	pole	0.09	1.473	1.638	$3.7 \cdot 10^3$	
9	pole	0.09	1.515	1.683	$4.7 \cdot 10^3$	
11	pole	0.09	1.548	1.720	$5.8 \cdot 10^3$	
15	pole	0.09	1.548	1.720	$5.8 \cdot 10^3$	
S = 42.2	H. yoke	0.102	1.548	1.515	$1.8 \cdot 10^3$	760
S = 15.0	V. yoke	0.096	1.548	1.610	$3.2 \cdot 10^3$	480
Total						36250

TABLE V

y cm	Part	Area m ²	Φ Weber	B Tesla	H A/m	NI At/pole
0-3	airgap			1.753	$6.8 \cdot 10^3$	41850
3	pole face	0.09	1.612	1.790	$8.0 \cdot 10^3$	} 4200
5	pole	0.09	1.713	1.903	$1.6 \cdot 10^4$	
7	pole		1.780	1.980	$2.4 \cdot 10^4$	
9	pole		1.832	2.035	$3.5 \cdot 10^4$	
11	pole		1.870	2.080	$5.2 \cdot 10^4$	
15	pole		1.870	2.080	$5.2 \cdot 10^4$	
S = 42.2	H. yoke	0.102	1.870	1.835	$1.0 \cdot 10^4$	4220
S = 15.0	V. yoke	0.096	1.870	1.950	$2.0 \cdot 10^4$	3000
Total						53270

The higher field values of Table V require 1100 amperes. The field homogeneity will not be the same as at the lower field, as the flux density in the pole edges goes up to 2.19 tesla, well above the saturation value of the iron. For many purposes the field may still be sufficiently good. The beam deflection would be 2 degrees at 45 GeV, 3 degrees at 30.0 GeV or 4 degrees at 22.6 GeV. If the temperature rise is 20°C at the rated current one would get 35° rise, still acceptable if the incoming water temperature is below 45°C.

For still higher currents and fields one would have to increase the water flow through the magnet.

Square copper conductors 0.590 inch \times 0.590 inch (15 mm \times 15 mm) with a 0.390 inch (10 mm) diameter hole are used, wrapped with glass fiber tape. After winding, each double pancake will again be wrapped with glass fiber tape and impregnated with epoxy. Due to the expected high radiation level in the beam switchyard, a radiation resistant epoxy shall be used. Materials that stand high temperature are in general also resistant to radiation. From this standpoint it has been specified that the insulation shall be class F (maximum working temperature 155°C). Tests indicate that this type of epoxy has acceptable mechanical and electrical properties after a dose of over 10^{12} ergs per gram. With reasonable precautions this should give more than 10 years lifetime.

The copper area of the conductor is 0.225 square inch (145 mm²) and the length per double pancake is 373 feet (114 meters). All pancakes will be connected in series electrically, in parallel for the water cooling.

E. OPTIMIZING DIMENSIONS

The selected dimensions are the result of a number of similar calculations with the same gap and pole width, but other dimensions slightly modified. In this way one can find an economic optimum design for a given performance. If, for instance, the yokes are made wider but the coils are unchanged, slightly less current is required for a given field in the gap. Assuming that the costs for power and iron are known, one can optimize the yoke width. The cost of power consists of a dominating cost for installation of HV-switchgear, transformers and rectifier with

high degree of stabilization (0.01%). It should also include the capitalized cost of energy over the expected life of the magnet. For this purpose the following values have been used:

Power at 220 kV 60 c/s	0.0075	\$/kWh
HV transformers and switchgear (at \approx 100% efficiency)	50	\$/kW
Rectifier with regulator and remote control (0.01% pre- cision and 90% efficiency)	$\left\{ \begin{array}{l} 120 \\ +1000 \end{array} \right.$	\$/kW
		\$/unit

The resulting cost for an increase in dc power is then

$$\text{Cost/kW} = 120 + \frac{50}{0.90} + \frac{0.0075}{0.90} T = 176 + 0.0084 T \quad (\$)$$

For an economic life of 5 years at 12 hours per day, 360 days per year and at an average 60% of rated current (= 36% of rated power), one finds

$$T = 5 \cdot 12 \cdot 360 \cdot 0.36 \text{ hours} = 7750 \text{ hours}$$

and

$$\text{Cost/kW} = 176 + 0.0084 \cdot 7750 \text{ \$/kW} = 240 \text{ \$/kW}$$

Cost for power	240	\$/kW
Cost for iron, machined	0.55	\$/lb
Cost for water-cooled coils per round of copper:		
Circular	2.50	\$/lb
Rectangular, simple	3.10	\$/lb
Curved (for large deflection angles)	3.80	\$/lb
With bent out ends for window type magnets tapered, complicated	4.00 - \$12.00	\$/lb

These cost values, based on magnet prices in USA 1962, would of course change with prices of raw materials and labor. As long as the ratio between the different costs remains essentially unchanged, about the same optimum dimensions will result. Near the optimum the change in total cost for a certain change in dimensions will be small and therefore the selection of dimensions is not too critical.

With given dimensions of the coil there is still freedom in the choice of number of turns in the winding. A small number of turns will increase the space factor and reduce the power and simplify the cooling system. It would, however, require a high current and heavy cables between the rectifier (or motor-generator) and the magnet. With an average distance of 300 feet one can estimate the cost of cables and installation including cable trays:

Cable cost 10 \$/ampere

The principal data of the magnet are given in Table VI.

TABLE VI

Total length of magnet	3.48 meters = 136.25 inches
Effective length	3.00 meters = 118 inches
Pole width	0.30 meters = 11.8 inches
Width of homogeneous field (10^{-3})	0.21 meters = 8.27 inches
Gap, 2h	0.06 meters = 2.36 inches
Number of turns per coil	48
Resistance at 55°C, coils in series	0.094 ohms
Voltage drop at 835A	78.5 volts
Power at 835A	65 kW
Field at 835A	1.55 tesla = 15,500 gauss
Water flow	0.78 kg/sec = 12.4 gpm
Pressure drop	4.36 atm = 62 psi
Temperature rise at 65 kW	20°C = 36°F
Weight, iron	12,000 kg = 26,400 pounds
copper	880 kg = 1,940 pounds
insulation, etc.	70 kg = 160 pounds
<u>Total</u>	12,950 kg = 28,500 pounds

LIST OF REFERENCES

1. M. E. Rose, "Magnetic field corrections in the cyclotron," Phys. Rev. 53, 715-719 (May 1938).
2. B. Hedin, "Design of CERN synchro-cyclotron magnet," CERN Report No. 55-3, European Council for Nuclear Research, Geneva, Switzerland (1955); p. 15.
3. E. Gerold, "Die abhängigkeit der magnetischen induktion bei baustählen von der chemischen zusammensetzung," Stahl u. Eisen 51, 613-15 (May 1931).
4. R. M. Bozorth, Ferromagnetism, D. van Nostrand, New York, New York (1951); p. 19 and p. 96.

LEGAL NOTICE

This report was prepared as an account of Government sponsored work. Neither the United States, nor the Commission, nor any person acting on behalf of the Commission:

A. Makes any warranty or representation, expressed or implied, with respect to the accuracy, completeness, or usefulness of the information contained in this report, or that the use of any information, apparatus, method, or process disclosed in this report may not infringe privately owned rights; or

B. Assumes any liabilities with respect to the use of, or for damages resulting from the use of any information, apparatus, method, or process disclosed in this report.

As used in the above, "person acting on behalf of the Commission" includes any employee or contractor of the Commission, or employee of such contractor, to the extent that such employee or contractor of the Commission, or employee of such contractor prepares, disseminates, or provides access to, any information pursuant to his employment or contract with the Commission, or his employment with such contractor.